JOURNAL OF CATALYSIS **161,** 507–516 (1996)
ARTICLE NO. 0212

The Influence of Support on the Low-Temperature Activity of Pd in the Reaction of CO Oxidation

2. Adsorption Properties and Reactivity of Adsorbed Species

S. N. Pavlova, V. A. Sadykov, V. A. Razdobarov, and E. A. Paukshtis

Boreskov Institute of Catalysis, Siberian Branch of the Russian Academy of Sciences, Novosibirsk, Russia

Received September 21, 1994; revised October 27, 1995; accepted January 24, 1996

Adsorption properties of Pd supported on γ-Al_2O_3, TiO_2, SiO_2, and adsorbed CO and oxygen low-temperature reactivities have been studied using IR spectroscopy, TPD, and pulse titration techniques. The results obtained are compared with the Pd surface structure data. At saturation coverages, weakly bound forms of CO (both linear and bridge-bonded) are the most reactive, their properties depending upon the type of support. Effect of Pd surface layer rearrangement due to CO and/or oxygen adsorption has also been found to be of importance. For mixed carbon monoxide–oxygen adlayer (θ_{CO} and θ_O are comparable), an overall Pd surface disordering occurs to wipe out all support effects.

INTRODUCTION

In the previous paper we investigated with TEM and EXAFS the structure and morphology of Pd particles supported on γ-Al_2O_3, TiO_2, and SiO_2 (1). We have found the structural parameters of Pd clusters to depend upon the nature of support, changing also under the influence of reaction media and/or its components. In this article we intend to compare the structural data with the Pd adsorption properties and reactivities of adsorbed species. Along with TPD and pulse titration techniques, we have also used IR spectroscopy to discriminate bonding strength and reactivities of linear and bridge-bonded carbonyls. Such a complex approach comes from the fact that local rearrangement of Pd particles under the action of CO and/or O_2 (2–4) makes elucidation of the active center nature at least quite challenging.

EXPERIMENTAL

The details of samples preparation (2.3% Pd/TiO_2, 2.6% Pd/Al_2O_3, 2.47% Pd/SiO_2) and some their characteristics are given in (1). In all kinetic and TPD experiments, a pulse/flow setup with a vibrofluidized bed microreactor were employed (5), helium being used as a carrier gas. For the pulse conditions, a relative pulse contact time (volume of a pulse divided by the volume rate of He) was ca 10 s. So in pulse experiments increasing the number of pulses increases the overall time of a catalyst contact with the reaction mixture. Reaction mixture components CO, CO_2, and O_2, were analyzed by gas chromatography (GC) with a thermal conductivity detector. All gases were purified by passing through traps cooled by liquid nitrogen.

Before kinetic and adsorption experiments, the catalysts (0.25–0.5 mm fraction) were reduced for 1 h in 30 cm^3/min of H_2 at 673 K. Following reduction the microreactor was purged with 60 cm^3/min He (<5 ppm O_2 admixture) at the same temperature for 30 min to remove H_2. The samples were cooled to the experiment temperature (257–298 K) in He.

Adsorbed CO and O_2 were titrated in a pulse manner with the mixtures containing 0.1–1% CO or 0.3–1% O_2 in He. For each experiment a fresh catalyst after standard pretreatment was used. The following series of experiments have been carried out:

I. Carbon monoxide adsorbed on the fresh Pd surface was titrated by oxygen pulses followed by a series of CO pulses to remove adsorbed oxygen,

1. $CO_{ads} + O_2(g)$
2. $O_{ads}(CO) + CO(g)$,

where $O_{ads}(CO)$ is used for oxygen adsorbed on the surface precovered by CO.

II. Oxygen adsorbed on the fresh Pd surface was titrated by carbon monoxide; thus, adsorbed CO was then titrated by oxygen pulses,

1. $O_{ads} + CO(g)$
2. $CO_{ads}(O) + O_2(g)$,

where $CO_{ads}(O)$ signifies carbon monoxide adsorbed on the surface precovered by oxygen.

0021-9517/96 $18.00

III. After the attainment of a stationary CO oxidation rate in the flow of reaction mixture, the catalyst was treated by pulses of either oxygen or CO,

1. $CO_{ads}(ss) + O_2(g)$
2. $O_{ads}(ss) + CO(g)$,

where $CO_{ads}(ss)$ and $O_{ads}(ss)$ stand for carbon monoxide or oxygen adsorbed on the steady-state catalyst surface. The rates were measured under essentially differential flow conditions (conversion, <10%). Reaction rate was defined as a number of CO_2 molecules evolved per 1 s from 1 m^2 of Pd surface.

The following procedure was used for the temperature-programmed desorption (TPD) of CO and oxygen. After standard pretreatment, a sample (1 g) was cooled to the adsorption temperature (253 K for CO adsorption and 298 K for oxygen adsorption) in a helium flow of 30 cm^3/min. Adsorption was carried out by passing 0.6% CO in He or pure oxygen flow of 30 cm^3/min through the catalyst bed to ensure saturation. The adsorption equilibrium was determined by the catharometer signal (6). The microreactor was then flushed for 10 min with He and TPD was performed in a stream of He at 20 K/min heating rate. In the TPD experiments, a trap filled with reduced MnO/SiO_2 was installed at the microreactor inlet providing a residual concentration of O_2 in He lower than several ppb.

The stepwise thermal desorption (STD) experiments were carried out to obtain information about CO forms held at the catalyst surface in the steady state of CO catalytic oxidation. For comparison with the TPD data, STD experiments were also carried out after CO adsorption on the fresh catalyst surface. Our routine TPD procedure required such big catalyst samples that it excluded catalytic rate measurements even at 253 K due to complete conversion of carbon monoxide. In STD experiments, the catalyst (50–100 mg) was pretreated in a usual way and cooled to 293 K in the He flow of 60 cm^3/min and then a flow (30 cm^3/min) of a reaction mixture ($CO + O_2$) or 1% CO in He was passed through the microreactor for 0.5–2 h. The sample was then purged with 60 cm^3/min of He at the same temperature for 1 min ("dead-time" interval required to wash out CO/O_2 from the microreactor). To collect at least a part of weakly bound CO and CO_2 easily desorbing at room temperature, on-line liquid nitrogen cooled traps filled with Ni–Cr wires and NaX zeolite were frozen immediately after dead-time and held frozen for 10 min. After consecutively warming up these traps, desorbed CO and CO_2 were analyzed by GC. In a further desorption experiment, the temperature was increased in steps of 50 K from 323 to 673 K. The traps freezing/warming and analysis procedures were identical at each temperature step.

The moles of CO and CO_2 desorbed in thermodesorption experiments were calculated from the GC data. Surface coverages were expressed as percentage of the Pd surface monolayer (monolayer was accepted to be equal to 10^{19} atoms) covered by CO or CO_2 molecules and calculated using specific surface values of supported Pd found from the TEM and oxygen adsorption data (1).

For infrared experiments, wafers with the densities of 10–30 mg/cm^2 (pressed at ~2.510^3 kg/cm^2) were used. They were placed in an IR cell that allows thermal treatments in the controlled atmosphere and in vacuum. The samples were reduced in H_2 (150 Torr) for 1 h at 673 K, evacuated at this temperature to ca. 10^{-4} Torr, and cooled to room temperature with a subsequent addition of 12–13 Torr CO. After IR spectra recording in 1800–2200 and 1200–1700 cm^{-1} regions on a UR-20 spectrometer, the samples were evacuated and oxygen (ca. 50 Torr) was added into the cell. After that the gas phase was removed and carbon monoxide was reintroduced into the cell, with spectra being recorded at each step.

RESULTS

Thermodesorption

Carbon monoxide and carbon dioxide. The TPD spectra of CO are given in Fig. 1. For Pd/TiO_2 the spectrum consists of three peaks located at 343, 413, and 643 K, the peak at 343 K being the most intense. A maximum at 343 K disappears completely after flashing by He at room temperature due to CO desorption.

For Pd/SiO_2 and Pd/Al_2O_3 the spectra are similar: a major part of CO desorbs at ~333–573 K. The most substantial differences are noticeable at low (<273 K) and high (>623 K) temperatures. The TPD spectrum for Pd/SiO_2 clearly shows a peak at 258 K, while the high-temperature peak at 633 K appears as a small shoulder. For Pd/Al_2O_3 the low-temperature peak at 293 K is weakly exposed as a shoulder, while the high-temperature peak at 663 K is very intense.

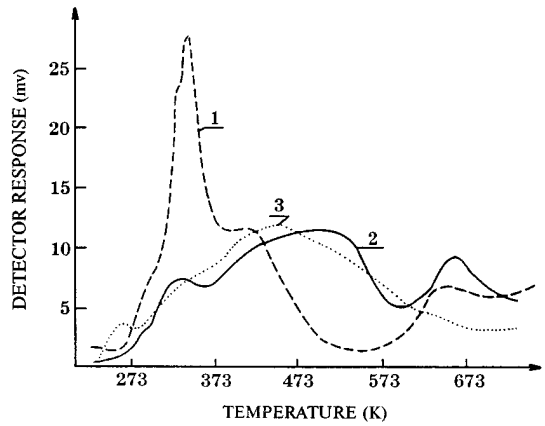

FIG. 1. TPD spectra for CO adsorbed on supported Pd at 253 K. 1, Pd/TiO_2; 2, Pd/Al_2O_3; 3, Pd/SiO_2.

TABLE 1

CO Thermodesorption Data for Bulk and Supported Pd

Sample	T_{max} (K)	Reference	T_{max} (K) (this work)
Pd (foil)	400 (sh.)	6	—
	513		
Pd(foil)	375	7	—
	615		
Pd/TiO_2	375	10	343
	523 (sh.)		413 (sh.)
	750		643
Pd/SiO_2	400	10	257
	488 (sh.)		323 (sh.)
	638		473
	777 (sh.)		513 (sh.)
			623 (sh.)
$Pd/\gamma\text{-}Al_2O_3$	393	12	293
	873		328
			413 (sh.)
			503
			663
$Pd/\alpha\text{-}Al_2O_3$	370	8	—
	450		

Table 1 compares our TPD results and the data published earlier (6–12). Evidently, if we pass from the bulk metal (single crystal faces (6), Pd-foil (7)) to supported catalysts (8–12), we see a considerable change in the distribution of the adsorbed CO forms. For Pd on the high surface area supports, the range of desorption temperatures expands: new forms with lower as well as higher desorption temperatures appear. It could seem natural to explain these phenomena by a high dispersion of supported Pd. However, in the case of small Pd clusters on a more or less inert support-basal plane of α-Al_2O_3, the peak positions at full coverages are nearly constant and identical to those for the Pd(111) face: 370 and 470 K (8). Hence, the size effect alone is not able to explain all the facts. At the same time (13), disordered Pd films prepared by vapor deposition were found to display a broad temperature range of CO desorption comparable with that observed here for Pd on the high-area supports. Hence, in the case of supported catalysts, defects could affect CO bonding strengths, though specific interaction with the chemically active supports might also be of importance (12). Thus, for our Pd/SiO_2 sample unique low-temperature form of adsorbed CO can originate from some kind of interaction with SiO_2 (possibly, decoration), which was revealed earlier by TEM (1).

The high-temperature peaks with $T_{max} > 700$ K can probably correspond to oxidation of the surface carbon by surface oxygen, both formed via CO_{ads} decomposition in the course of heating up to 473–573 K. Indeed, according to Popova *et al.* (12) and Palazov *et al.* (14), the degree of CO disproportionation on supported Pd significantly increases as the adsorption temperature increases. Clearly, CO decomposition requires sites with high affinity to carbon and oxygen unusual for regular Pd atoms on the single crystal planes. TPD peaks at ~473–523 K imply adsorption centers more strongly binding CO than those on the (111) face, adsorption being reversible in this case (Fig. 1).

The results of STD experiments are shown in Fig. 2. For the case of CO adsorbed on the fresh Pd surface, they agree with the TPD data: temperatures of the most intense $CO(CO_2)$ evolution more or less coincide in both sets of experiments. The integral coverages of Pd surface by carbon monoxide (calculated from the sum of CO and CO_2 evolved) attained after catalyst contacting with various gas mixtures are collected in Table 2. The value of θ_{CO} obtained for fresh Pd/TiO_2 in the STD experiments differ considerably from that derived from the TPD data. According to the latter, for all three catalysts θ_{CO} is close to 1, while STD for Pd/TiO_2 gives θ_{CO} ca. 0.5–0.6. These discrepancies could be assigned to different temperatures of adsorption: 253 K for TPD and 293 K for STD. For fresh Pd/TiO_2, a weakly bound CO desorbing even at room temperature can be detected only starting TPD at temperatures below 273 K. On the other two supports, the surface of palladium particles is almost completely covered by CO even at room temperature,

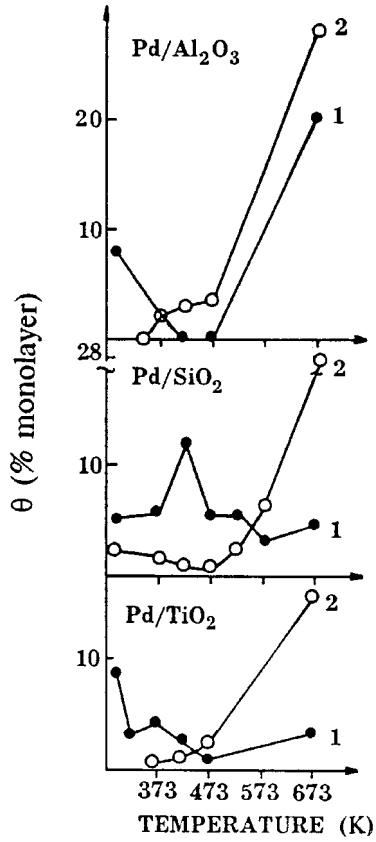

FIG. 2. STD spectra for CO and CO_2 after CO adsorption on fresh catalysts. 1, CO; 2, CO_2.

TABLE 2

Integral Coverages of Pd Surface by CO and CO_2

Catalyst	Integral coverage (% of monolayer)			
	TPD	STD	STD for steady-state	
Pd/TiO_2	98	42	82[a]	52[b]
Pd/Al_2O_3	95	95	110[a]	110[b]
Pd/SiO_2	110	98	—	120[b]

[a] Reaction mixture composition, 1% CO + 1% O_2 in He.
[b] Reaction mixture composition, 1% CO + 19% O_2 in He.

save for the low-temperature form on Pd/SiO_2 (*vide supra*).

For all catalysts with both TPD and STD, we have observed a considerable CO_2 evolution (see Figs. 2 and 3). In general, CO_2 formation can proceed via several routes: (i) through disproportionation, $2CO_{ads} \rightarrow C_{ads} + CO_2$; (ii) via CO interaction with oxygen captured by Pd from the He stream; (iii) a water–gas shift reaction; (iv) decomposition of the surface formate species. We can exclude the two last routes due to lack of hydrogen in the helium stream at the reactor outlet. Note the different conditions of TPD and STD experiments: at TPD the weights of catalysts are considerably higher and the level of O_2 admixture in He is substantially lower, while at STD an increased time of desorption (ca. hours) and a higher level of oxygen in He (~ppm instead of ppb) enhance the amount of oxygen captured by Pd. The estimations based on the oxygen balance in the helium stream have shown that at TPD CO_2 is formed via disproportionation, while at STD it is due to CO oxidation by a captured oxygen. A feeding of the oxygen pulses onto the samples after CO desorption has confirmed that at STD a possible amount of carbon formed in the course of adsorption–desorption is quite low, not exceeding 7% of monolayer.

The STD spectra for samples treated at room temperature by reaction mixture or after successive adsorption of

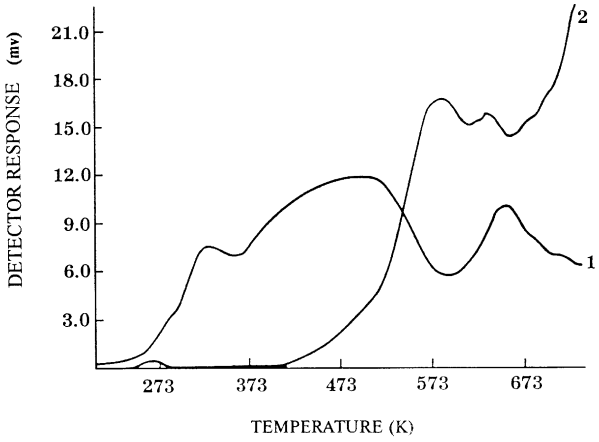

FIG. 3. TPD spectra for CO and CO_2 on Pd/Al_2O_3. 1, CO; 2, CO_2.

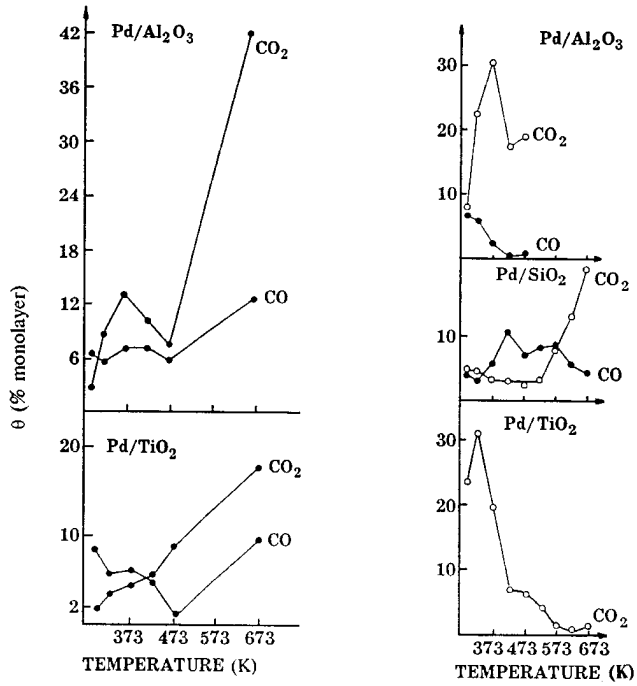

FIG. 4. STD spectra for CO and CO_2: (a) after successive adsorption of O_2 and CO at 298 K, (b) after attainment of a steady-state activity in the flow of 1% CO + 19% O_2 in He mixture at 298 K.

O_2 and CO are shown in Fig. 4, the corresponding integral CO coverages are listed in Table 2. In these experiments CO_2 is evolved due to a surface reaction $CO_{ad} + O_{ad}$. For Pd/SiO_2 the spectra are similar to those obtained after CO adsorption (Fig. 2) but an increased amount of CO_2 evolved at low temperatures. For Pd/Al_2O_3, a small amount of CO desorbs at low temperatures while a high-temperature form is absent. For this catalyst the major part of the initially adsorbed CO desorbs in the form of CO_2 with T_{max} ca. 373 K both for the steady-state and after successive adsorption of O_2 and CO (Fig. 4), while the amount of evolved CO_2 is higher for the former case: Pd is more oxidized. In contrary, for the single crystal faces of Pd precovered by oxygen the increase of CO exposures shifts T_{max} of CO_2 peak from 480 to 300 K. This is accompanied by the decrease of CO_2 evolved due to oxygen titration by CO even at room temperature (15). Such shift of T_{max} is explained by change of the CO and O_2 spatial distribution in the adlayer (15). For supported Pd (*vide infra*), the most part of adsorbed oxygen is also titrated by the gas-phase CO, but here T_{max} is nearly constant. Since T_{max} at high CO exposures is higher for the case of supported Pd, it may be safely suggested that oxygen not titrated by CO at ambient temperatures is less reactive than that chemisorbed on the single crystal faces. Such a difference could be explained by incorporation of oxygen into the subsurface layer, which was clearly monitored by EXAFS for palladium on silica and alumina (1). Hence, for

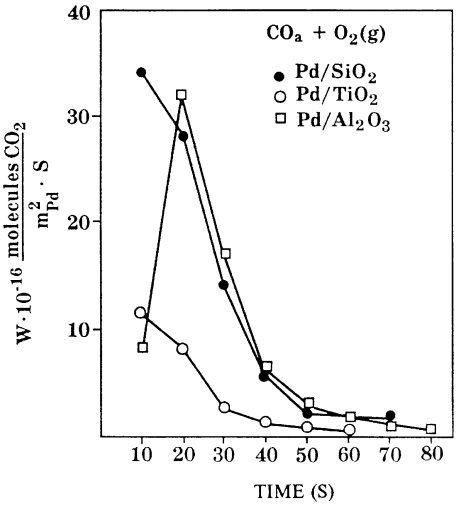

FIG. 5. The rate of CO_2 evolution during titration of CO adsorbed on freshly reduced Pd surface by pulses of 1% O_2 in He at 298 K.

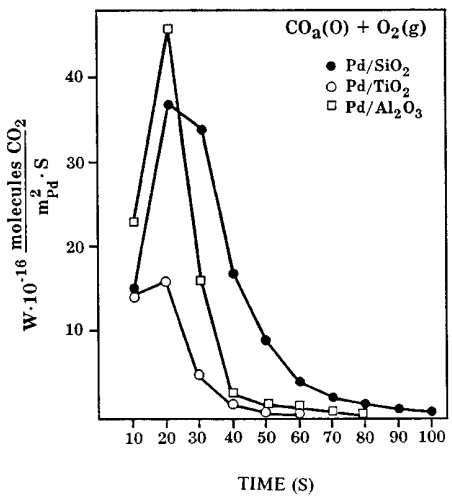

FIG. 6. The rate of CO_2 evolution during titration of CO adsorbed on Pd surface precovered by oxygen. 1% CO in He and 1% O_2 in He mixtures were used for adsorption and titration at 298 K.

Pd on these supports in the steady-state surface adlayer, carbon monoxide, and oxygen are spatially separated.

For Pd/TiO_2, oxygen preadsorption increases the sum of the amounts of CO and CO_2 desorbed in STD experiments up to a monolayer value. For a steady-state of Pd/TiO_2 , only CO_2 is evolved there ($T_{max} \sim 323$ K, Fig. 4), suggesting the adsorbed layer to consist of mixed CO and oxygen structures. The relationship between CO coverage and oxygen content in the reaction mixtures (Table 2) favors this assumption.

Oxygen. For all three catalysts investigated thermodesorption has revealed a low-temperature form of oxygen ($T_{max} = 373$ K) constituting 1–3% of monolayer. This form is absent on the bulk Pd at all adsorption temperatures (16–18), any oxygen desorption being observed only at $T > 600$ K. For Pd supported on γ-Al_2O_3, a peak of a relatively weakly bound molecular oxygen ($T_{max} \sim 423$ K, $E_{des} \sim 5.5$–7.7 kcal/mol) was registered only if adsorption temperatures were higher than 423 K (12). Therefore, for our catalysts the state of adsorbed oxygen differs considerably from those typical for bulk Pd or Pd supported on γ-Al_2O_3.

Reactions of CO and Oxygen Titration

Figure 5 shows the curves of adsorbed CO titration by gas-phase oxygen for the fresh Pd surface. For Pd/SiO_2 and Pd/TiO_2 samples, the rate of CO_2 evolution versus time is of s-type, maximum being attained in the first pulse. In the case of Pd/Al_2O_3, CO_2 readsorption on the support decreases CO_2 evolution in the first pulse, so $W(CO_2)$ reaches a maximum only at the second pulse. For this catalyst CO_2 preadsorption was found to make the titration curve identical to those for the other samples. In contrast, low-temperature titration of CO adsorbed on the single crystal faces (15) or coarse-particled Pd supported on alumina (19) has a pronounced induction period typical for the Langmuir–Hinshelwood mechanism of this reaction. Hence, for small clusters of supported Pd weakly bound CO detected in the TPD experiments does demonstrate high reactivity, thus changing the shape of the titration curve.

The data for titration of carbon monoxide adsorbed on the surface precovered by oxygen are given in Fig. 6. For all three catalysts, the curves of CO_2 evolution versus time of reaction go through the maximum. The most significant difference between the initial and the maximum rates of CO_2 evolution was observed for Pd/SiO_2 and Pd/Al_2O_3. At the same θ_{CO}, the rate of CO_2 evolution was found to depend upon the gas-phase oxygen concentration that implies a possible contribution of a quasi-impact type route

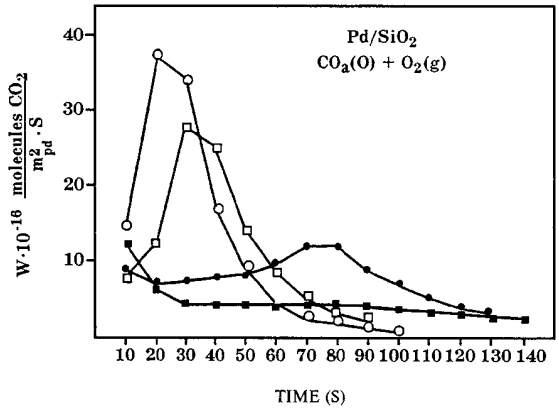

FIG. 7. The rate of CO_2 production during the titration of CO adsorbed on the surface of Pd/SiO_2 precovered by oxygen. Mixtures of 1% CO or 1% O_2 in He were used at the following temperatures: 298 K (open circles); 273 K (solid circles); 257 K (solid squares). Mixtures of 0.3% O_2 or 0.1% CO in He were used at 298 K (open squares).

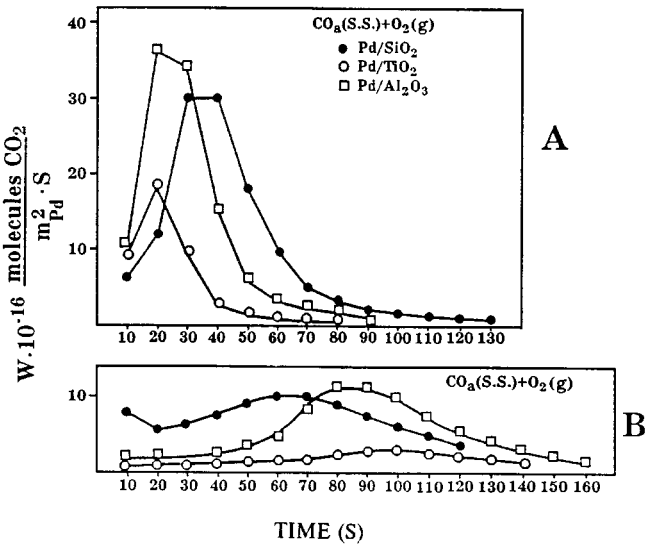

FIG. 8. The rate of CO_2 production during titration of CO adsorbed on the surface of Pd after attainment of a steady-state activity in the flow of 1% CO + 19% O_2 in He: (A) 293 K, (B) 273 K.

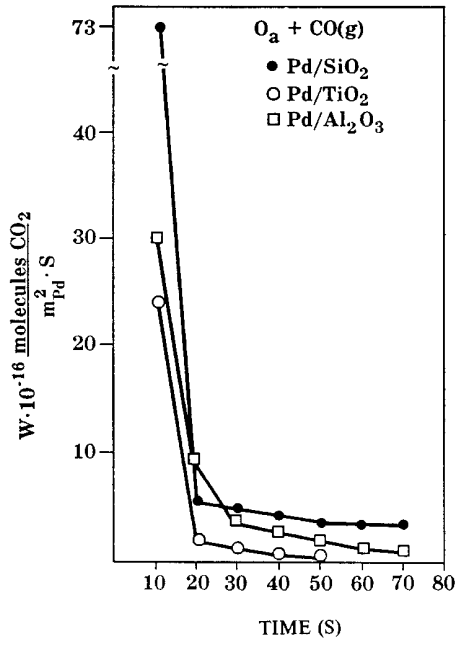

FIG. 9. The rate of CO_2 evolution during titration of oxygen adsorbed on the freshly reduced Pd surface by pulses of 1% CO in He.

($CO_{ads} + O_{2gas}$). Similar dependencies were also obtained at lower temperatures (Fig. 7), while titration curves flattened. Initial portions of these curves for Pd/SiO_2 at 273 and 257 K (Fig. 7) have some peculiarities: a pronounced minimum appears and the initial rate decreases while temperature increases. These features prove existence of at least two distinct states of adsorbed CO sharply differing by their reactivity, a weakly bound form easily desorbing around 273 K (*vide supra*) being the most reactive.

In the case of carbon monoxide adsorbed on the steady-state catalyst surface, the titration curves also have distinct maximum (Fig. 8). The influence of the reaction media is rather well manifested by a pronounced fall of the initial rates of CO titration as compared with those for CO adsorbed on fresh surface. At 298 K, maximum titration rates normalized to the initial CO coverage (compare the data of Fig. 8 and Table 2) are nearly support-independent.

The curves of adsorbed oxygen titration by pulses of CO in He are presented in Figs. 9 and 10. Irrespective of the mode of the oxygen adlayer formation, the rate of interaction between the adsorbed oxygen and gas-phase carbon monoxide monotonously decreases from pulse to pulse. For Pd/Al_2O_3 $W(CO_2)$ in the first pulse is somewhat underestimated due to CO_2 readsorption on the support. If this phenomenon is taken into account, a corrected initial rate of CO_2 evolution for this sample is close to that for Pd/SiO_2. An observed mode of $W(CO_2)$ variation is formally described by the mechanism of an impact type, though in fact mixed CO–oxygen islands may be formed (20). For the Pd single-crystal planes the situation is more complex than for supported catalysts and depends upon the face type. In the case of the (111) face, a pronounced induction period was observed even for temperatures around 323 K indicating the Langmuir–Hinshelwood route (15), whereas for the (110) face at 363 K initial titration rates were the highest (19). It seems that namely disordering of the surface layer of small clusters by oxygen adsorption revealed by EXAFS (1) determines its enhanced reactivity.

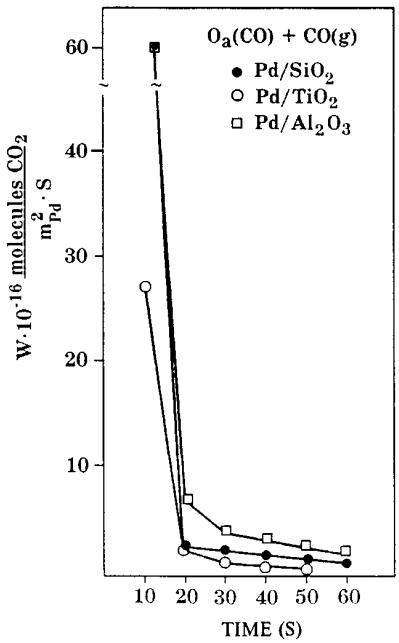

FIG. 10. The rate of CO_2 evolution during the titration of oxygen adsorbed on the surface of catalysts precovered by CO. Gas mixtures: 1% CO or 1% O_2 in He; 298 K.

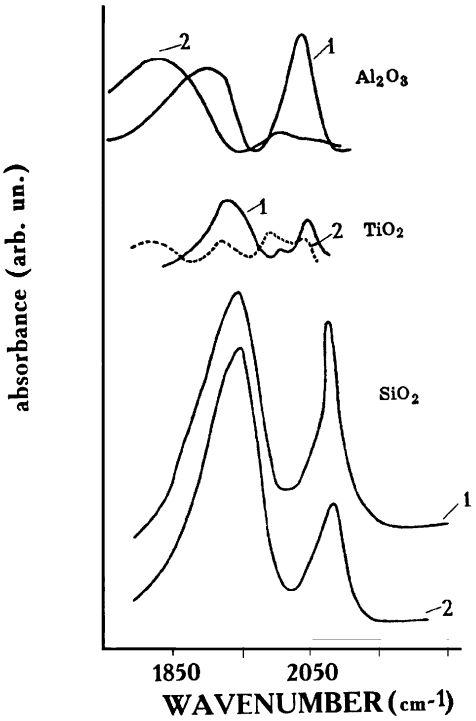

FIG. 11. IR spectra of CO adsorbed on 2.47% Pd/SiO_2, 2.6% Pd/Al_2O_3, 2.3% Pd/TiO_2. $T_{ads} = 298$ K. 1, at $P_{CO} = 10$ Torr; 2, after evacuation at 298 K.

IR Spectra of Adsorbed CO

Figure 11 shows the spectra of CO adsorbed at room temperature (actually at ca. 323 K because of the heating effect of the beam). Several features are especially worthy of comment:

(1) For samples studied here the ratio of the intensities of linear (absorption bands at ~2080–2090 cm^{-1}) and bridge-bonded (absorption bands at ~1980–1990 cm^{-1}) carbonyls (14) varies only slightly. Hence, in our case decoration of the Pd clusters by TiO_x species usually manifested by an increase of the relative abundance of linearly bonded CO (21) seems to be not essential. This result is in a general agreement with the TPD data for this sample (*vide supra*), indicating a nearly monolayer coverage of Pd surface by CO at 273 K. As judged from the enhanced relative intensity of linear carbonyls for our Pd/SiO_2 and $Pd/\gamma\text{-}Al_2O_3$ samples as compared with samples of higher Pd loadings (14, 21), decoration would be well expected for these two supports. Probably, decoration could arise due to migration of the hydrated fragments of a support onto the metal particles (23). Our estimations based upon the chemisorption data show that decoration, if any, is limited to no more than 5–10% of Pd monolayer.

(2) The Pd/TiO_2 catalyst displays the broadest variation in the nature of centers adsorbing CO in linear form that is seen from the splitting of the band of linear CO ($\delta\nu \sim 30$ cm^{-1}). A similar but less pronounced phenomena (splitting ~10 cm^{-1}) was observed for small (ca. 10 Å) Pd clusters on SiO_2 (11) and $\gamma\text{-}Al_2O_3$ (24). Since linear form is usually assigned to CO adsorbed on defect centers, these results agree well with the EXAFS data (1) implying that the highest disordering of the surface of Pd/TiO_2 is due to CO adsorption. For reduced Pd/TiO_2, the band of the bridge-bonded CO is nearly symmetric and could be assigned to carbon monoxide located on the (110) or (100) faces, while more tightly bound and less reactive form with lower ν_{CO} (~1920 cm^{-1}) assigned to adsorption on the (111) type faces (25, 26) is absent. Hence, the IR data confirm anisotropy of the Pd clusters on TiO_2 due to epitaxy with this support (1).

(3) The intensity of linear-bonded CO adsorbed on Pd/SiO_2 and Pd/Al_2O_3 quickly falls at cell evacuation while bridge-bonded CO remains on the surface (Fig. 11). Therefore, for these catalysts a weakly bound form is of a linear type, which agrees with the results of (14, 23). Carbon monoxide adsorbed on Pd/TiO_2 exhibits quite different properties: both forms are easily desorbed at room temperature, thus demonstrating comparable (and low) bonding strength. Earlier, a similar phenomenon was observed for Pd on such support as La_2O_3 (23), which was explained by a weakening in the σ component of the Pd–CO bond due to a charge transfer from the partially reduced lanthana to Pd crystallites. However, such effect seems not to operate here. Indeed, for Pd/TiO_2 and Pd/SiO_2 (prepared by the same procedure as in our work) Lokhov and Bredikhin (27) have proved singletons (ν_{CO} at $\theta_{CO} \to 0$) for two-bonded and three-bonded CO to be identical and equal to 1895 cm^{-1} and 1805–1810 cm^{-1}, respectively. Singletons are known to be a function of the electron density on the metal. Therefore, any specific electron charge transfer between the reduced TiO_2 and Pd clusters is hardly probable here.

(4) To estimate reactivities of various forms of adsorbed CO (carbonyls located on Pd atoms and carbonate–carboxylate complexes stabilized by support), room-temperature titration of ad-CO_x by gas-phase oxygen in the IR cell has been carried out; the results are given in Figs. 12–14. Absorbance in the 1350–1750 cm^{-1} is usually assigned to carbonate–carboxylate complexes; band positions and relative intensities observed here are in a reasonable agreement with the results of (28, 29). These species have a negligible reactivity: their intensities increase only after oxygen admission due to CO_2 readsorption. For Pd/TiO_2 and Pd/Al_2O_3 both bridged and linear carbonyls are very reactive. A typical time of their consumption by the gas-phase oxygen found here (~minute) agrees well with the results of pulse experiments (*vide supra*). For Pd/SiO_2 linear CO has higher reactivity than the bridged form (Fig. 12), which correlates with their relative bonding strength.

(5) CO adsorption after oxygen preadsorption (Figs. 13 and 14) has revealed that soft oxidation of the surface of supported Pd is not accompanied by the appearance of any

absorption bands at higher frequencies which could be assigned to CO complexes with Pd^{1+} and Pd^{2+} ions, which agrees well with the results of (14, 19). This fact is easily explained by rapid titration of adsorbed oxygen by carbon monoxide with typical times of approximately 1 min (*vide supra*). More subtle effects probably caused by oxygen incorporation into the subsurface layer substantially differ for Pd/TiO_2 and other two samples. For the first sample the integral intensity of adsorbed CO increases considerably after O_2 preadsorption, which is in excellent agreement with our STD data (nearly twofold increase in θ_{CO} for Pd/TiO_2 preoxidized at room temperature). Moreover, the band of bridged-bonded CO becomes asymmetric due to emerging of the low-frequency shoulder (usually a more tightly bound and less reactive form (26)). For the other two samples the oxygen preadsorption decreases the relative intensity of linear form and somewhat enhances the intensity of bridged form (cf. Fig. 13 for Pd/Al_2O_3). Therefore, for these catalysts the initial rate of CO titration after oxygen preadsorption (*vide supra*) falls due to both increase of θ_{CO} and decline of the most reactive linear form coverage. Possible explanation of the phenomena observed could stem from Pd surface restructuring caused by oxygen incorporation (22). Note that for the samples with lower Pd dispersions and higher (ca. 9%) loadings the picture is somewhat different: incorporation of oxygen into the subsurface layer is accompanied by an increase in the intensity of linear form (very weakly exposed in fresh sample) and growth of the low-temperature activity in CO catalytic oxidation (22).

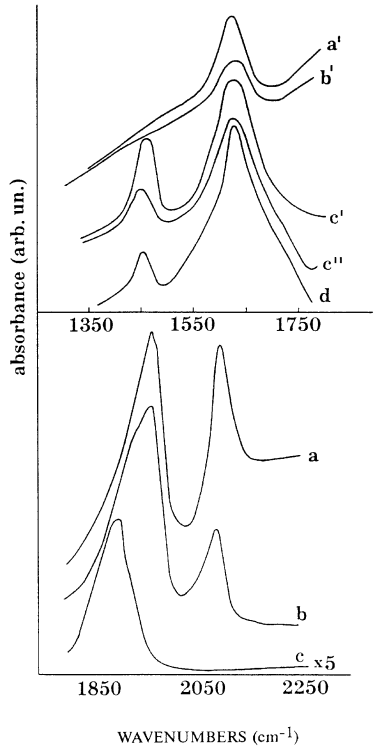

FIG. 12. IR spectra of CO adsorbed on 2.47% Pd/SiO_2. $T = 298$ K. a,a′, CO adsorbed at $P_{CO} = 10$ Torr; b,b′, after evacuation at 298K; c,c′, immediately after addition of O_2 ($P = 50$ Torr); c″, after 30 min; d, subsequent CO adsorption at $P_{CO} = 10$ Torr after gas-phase oxygen pumping.

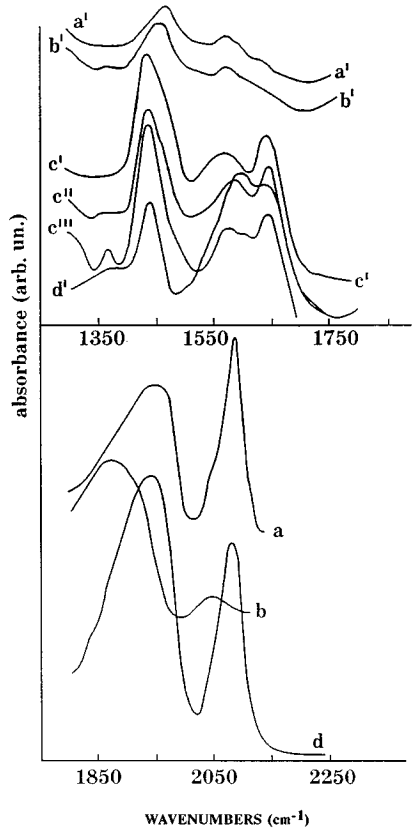

FIG. 13. IR-spectra of CO adsorbed on 2.6% Pd/Al_2O_3. $T = 298$ K. a,a′, CO adsorbed at $P_{CO} = 10$ Torr; b,b′, after evacuation at 298 K; c′, immediately after addition of O_2 ($P = 50$ Torr); c″, after 20 min; c‴, after 40 min; d,d′, subsequent to adsorption at $P_{CO} = 10$ Torr after gas-phase oxygen pumping.

DISCUSSION

The Effect of Support on CO Bonding Strength

Thermodesorption and IR spectroscopy data show substantial variation of CO bonding and saturation coverages as dependent upon the type of support. Weakly bound CO forms can be assigned to both linear and bridge-bonded carbonyls; the latter is rather unexpected. Two factors seem to be responsible for the appearance of these weakly bound states:

(1) Steric effect caused by dilution of CO adlayer due to Pd surface decoration by support species (9, 10). In our case it is restricted to 5–10% of monolayer and mainly operates for Pd supported on γ-Al_2O_3 and SiO_2. As well as generating linear forms of CO, these MeO_x species also decrease CO bonding strength as compared with the single crystal

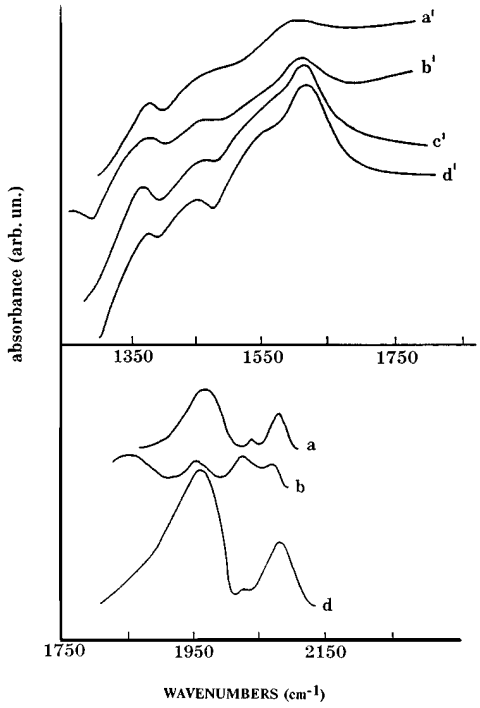

FIG. 14. IR spectra of CO adsorbed on 2.3% Pd/TiO_2. $T = 298$ K. a,a′, $P_{CO} = 10$ Torr; b,b′, after evacuation at 298 K; c′, immediately after addition of O_2 ($P = 50$ Torr). d,d′, subsequent CO adsorption at $P_{CO} = 10$ Torr after gas-phase oxygen pumping.

data. Possibly, the presence of highly charged ions (Si^{4+}, Al^{3+}) in the coordination sphere of Pd atom influences its mode of interaction with CO via some electrostatic or geometric effects.

(2) Effects due to reconstruction of the open type (100) and (110) Pd faces into more dense corrugated layers with a local hexagonal arrangement of Pd atoms (30, 31). The driving force for this process is coordinative unsaturation of the clean Pd surface. When CO is adsorbed, a reverse process takes place accompanied by corresponding Pd–Pd bond redistribution (31). Such type of Pd structure disordering both for clean surfaces and under effect of adsorbed gases was earlier implied from EXAFS data (1). As would be expected, such effects are the most pronounced for flat Pd clusters on TiO_2, where due to epitaxy with this support, Pd surface faces of the (110) type are the most developed.

First of all, these processes of reconstruction typical for flexible surfaces (31) can influence the heats of CO and oxygen adsorption via generation of new types of defect centers. Further, in the frames of the concerted mechanism of CO/O_2 adsorption, enthalpies of relaxation processes (formation/rupture of the Pd–Pd bonds) can be directly included in the heats of adsorption (32, 32). Oxygen incorporation into the subsurface layer appears to affect these processes of relaxation, thus strengthening Pd–CO bonds.

Hence, several types of mechanisms seem to operate in support effect on the bonding strength of CO adsorbed on Pd particles. For a given support, one or another type can dominate as dependent upon the support nature. First of all, it is decoration probably coupled with some kind of the electrostatic effects. Second, due to epitaxy, support can stabilize certain types of surface faces with various structures and abilities to reconstruct. The last one is that support can facilitate oxygen incorporation into the subsurface layers of Pd.

From the point of view of the surface science, all these mechanisms operate via changing defect structure of the Pd surface. Support specificity thus somewhat restricts flexibility of the small Pd particle structure at ambient temperature, thus allowing one to observe all effects considered above. Otherwise, disordering caused by adsorbed gases could completely remove all initial structural differences of supported Pd.

Reactivity of Adsorbed Species

Titration experiments and IR data have demonstrated that under the unsteady-state conditions adsorbed carbon monoxide and oxygen are very reactive. As could be suggested from the observed pressure dependence of the initial titration rates, at high CO coverages a considerable part of CO_2 is produced via a quasi-impact type route ($CO_{ads} + O_{2gas}$). For freshly reduced surface of Pd, an s-type titration curve seems to indicate the coexistence of the impact and adsorption types of mechanism in the whole range of coverages, while for a preoxidized or steady-state surface the adsorption mechanism clearly dominates. The term "adsorption mechanism" does not imply the reaction in an ideal adsorption layer. The surface could be microheterogeneous, covered by patches of pure or mixed structures with reaction occurring at their boundaries (11, 20, 33). Moreover, a variety of centers exists at the reconstructed surfaces. Similarly, quasi-impact type features can be observed when reactive atomic forms of oxygen adsorbed on defect centers are in equilibrium with the molecular oxygen. The physical reason for such enhanced reactivity of CO adsorbed on small particles of supported Pd appears to be high density of surface defect centers stabilizing weakly bound forms (*vide supra*). First of all, it is reflected in support sensitivity of the initial titration rates especially at low temperatures. The second phenomenon worth mentioning is a general disordering of the supported Pd particles under the action of the reaction mixture components (CO and oxygen) revealed by EXAFS. It appears also to be reflected in the titration experiments. Thus, at 293 K the maximum rates of CO titration on a steady-state surface are support-independent. The activation energies of the surface reaction $CO_{ads} + O_{ads}$ estimated from the temperature dependence of W_{max} by analogy with (15) were also found to be practically identical for Pd on various supports (33–42 kJ/mol) and substantially lower than in the case of bulk metal (58 kJ/mol). Our estimations show that at room temperature the maximum rate

of surface reaction for supported Pd is about two orders of magnitude higher than that for single crystals and bulk Pd.

It seems that even in the course of CO titration, some incorporation of oxygen into the subsurface layer occurs, thus generating strong distortion of the surface. As the result, all initial structural differences are washed out (34), so that the binding energy of adsorbed CO, activation energy of surface reaction, and its turnover rate become insensitive to the nature of Pd–support interaction. At the same time, at $\theta_{CO} \sim 1$ TPD spectra and CO titration curves retain specificity even in the presence of the subsurface oxygen.

Therefore, reactivity of CO adsorbed on supported Pd is greatly enhanced, all CO being reactive at room temperature due to both genetic and induced defects. The same is true for the adsorbed oxygen. This trend is undoubtedly less expressed for bulk Pd (single crystals, foils).

Our data seem to demonstrate the absence of any low-temperature reactivity of the carbonate–carboxylate complexes stabilized by supports. A contradiction with the conclusions of a number of earlier papers (12, 35–37) could be explained by a higher dispersion of their samples leading to stabilization of the oxidized forms of Pd incorporated in the vacancies of γ-Al_2O_3. These ions could retain carbonate–carboxylate complexes of increased reactivity.

CONCLUSIONS

At saturation coverages of small supported palladium particles by carbon monoxide the most reactive weakly bound forms of CO (both linear and bridge-bonded) appear to be mainly located at defect centers generated by reconstruction of the open (100) and (110) faces. Defect center density was found to depend upon the mode of palladium particle interaction with a support (epitaxy, decoration, etc.). Oxygen incorporation into the subsurface layer seems to suppress the surface reconstruction, thus decreasing a number of defect centers. For mixed carbon monoxide–oxygen adlayer (at comparable θ_{CO} and θ_O) an overall disordering of the palladium surface occurs, wiping out all support effects. Hence, at $\theta_{CO} \sim \theta_O \sim 0.5$ the maximum rate of CO titration by gas-phase oxygen was found to be support-independent and higher than that for bulk Pd.

ACKNOWLEDGMENT

The authors are grateful to Savchenko V. I. for valuable discussion.

REFERENCES

1. Kochubei, D. I., Pavlova, S. N., Novgorodov, B. N., Kryukova, G. N., and Sadykov, V. A., *J. Catal.,* **161**, 500 (1996).
2. Gaussman, A., and Kruse, N., *Catal. Lett.* **10**, 305 (1991).
3. Hevine, R. D., and Somorjai, G. A., *Surf. Sci.* **232**, 407 (1990).
4. El-yakhloufi, M. N., and Gillet, E., *Catal. Lett.* **17**, 11 (1993).
5. Veniaminov, S. A., and Barannik, G. V., *React. Kinet. Catal. Lett.* **13**, 413 (1980).
6. Ertl, T., and Koch, J., *in* "Proceedings, 5th International Congress on Catalysis, Palm Beach, 1972" (J. Hightower, Ed.). Noth-Holland, Amsterdam, 1973.
7. Close, H., and White, J., *J. Catal.* **36**, 185 (1975).
8. Ladas, S., Poppa, H., and Boudart, M., *Surf. Sci.* **102**, 151 (1981).
9. Rieck, J. S., and Bell, A. T., *J. Catal.* **103**, 46 (1987).
10. Rieck, J. S., and Bell, A. T., *J. Catal.* **99**, 262 (1987).
11. Ichikawa, S., Poppa, H., and Boudart, M., *J. Catal.* **91**, 1 (1985).
12. Popova, N. M., Babenkova, L. V., and Savelyeva, G. A., *in* "Adsoption and Interacion of The Simplest Gases with Metals of the 8th Group." Nauka, Alma-Ata, 1979. [In Russian]
13. Stephan, J. J., Franke, B. L., and Ponec, V., *J. Catal.* **44**, 359 (1976).
14. Palazov, A., Chang, C., and Kokes, J., *J. Catal.* **36**, 338 (1975).
15. Conrad, H., Ertl, T., and Kuppers, J., *Surf. Sci.* **76**, 323 (1978).
16. Conrad, H., Ertl, G., Kuppers, J., and Latta, E. E., *Surf. Sci.* **65**, 245 (1977).
17. Weissman, P., Shekand, M., and Spiser, W., *Surf. Sci.* **92**, 159 (1980).
18. Savelieva, G. A., Beshenei, P. G., Smirnova, H. G., Popova, N. M., Shvets, V. A., Sass, A. S., Galeev, G. K., Shubin, V. E., and Kazanskii, V. B., *Kinet. Katal.* **25**, 670 (1984). [in Russian]
19. Ladas, S., Imbil, P., and Ertl, G., *Surf. Sci.* **280**, 14 (1993).
20. Zhou, X., and Gilari, E., *Langmuir* **2**, 709 (1986).
21. Bredikhin, M. N., Lokhov, Yu. A., and Zamarayev, K. I., *Dokl. AN SSSR.* **301**, 1124 (1988). [in Russian]
22. Hicks, R. F., Qi, H., Kooh, A. B., and Tisehel, L. B., *J. Catal.* **124**, 488 (1990).
23. Hicks, R. F., Qi-Jie Yen, and Bell, A. T., *J. Catal.* **89**, 498 (1984).
24. Yuszczyk, W., Karpinski, Z., Ratajczykova, I., Stanasiuk, Z., and Zielinski, J., *J. Catal.* **120**, 68 (1989).
25. Sheppard, N., and Nguyen, T. T., *in* "Advances in Infrared and Raman Spectroscopy" (B. J. H. Clark and B. E. Hester, Eds.), Vol. 5. Heyden and Sons, London, 1978.
26. Palazov, A., Kadinov, G., Bonev, Ch., and Shopov, D., *J. Catal.* **74**, 44 (1982).
27. Bredikhin, M. N., and Lokhov, Yu. A., *J. Catal.* **115**, 601 (1989).
28. Haruta, M., Tsubota, S., and Kobayashi, T., *in* "Proceedings, 10th Internatrional Congress on Catalysis, Budapest, 1992" (L. Guczi, F. Solymosi, and P. Tetenyi, Eds.). Akadémiai Kiadó, Budapest, 1993.
29. Savelyeva, G., A., Sass, A. S., and Popova, N. M., *Zh. Fiz Khim.* **62**, 1021 (1988). [in Russian]
30. Heinz, K., *Surf. Sci.* **299/300**, 433 (1994).
31. Somorjai, G. A., *in* "Annual Review of Physics and Chemistry," Vol. 45, p. 721 Annual Reviews, Palo Alto, CA, 1994.
32. Engel, T., and Ertl, G., *in* "Advances in Catalysis," Vol. 28, p. 1. Academic Press, New York, 1975.
32. Galeev, T. K., Bulgakov, N. N., Savelyeva, G. A., and Popova, N. M., *React. Kinet. Catal. Lett.* **14**, 55 (1980).
33. Tikhov, S. F., Sadykov, V. A., Kryukova, G. N., Paukshtis, E. A., Popovskii, V. V., Starostina, T. G., Kharlamov, G. V., Anufrienko, V. F., Poluboyarov, V. F., Razdobarov, V. A., Bulgakov, N. N., and Kalinkin, A. V., *J. Catal.* **134**, 506 (1992).
34. Engel, T., and Ertl, G., *in* "Advances in Catalysis," Vol. 28, p. 1. Academic Press, New York, 1975.
35. Savchenko, V. I., Thesis ... dokt. naul. Novosibirsk, Institute of Catalysis, 1985. [in Russian]
36. Conrad, H., Ertl, G., Conrad, J., and Latta, E. E., *Surf. Sci.* **43**, 46 (1974).
37. Moorhead, R. D., Poppa, H., and Dickkinson, J. T., *J. Vac. Sci. Technol.* **17**, 198 (1980).
38. Fajula, F., Antony, R. G., and Lunsdorf, J. M., *J. Catal.* **73**, 237 (1982).